A LETTERS JOURNAL EXPLORING
THE FRONTIERS OF PHYSICS

OFFPRINT

Joint downscale fluxes of energy and potential enstrophy in rotating stratified Boussinesq flows

H. ALUIE and S. KURIEN

EPL, **96** (2011) 44006

A Letters Journal Exploring the Frontiers of Physics

November 2011

EPL, **96** (2011) 44006 www.epljournal.org
doi: 10.1209/0295-5075/96/44006

Joint downscale fluxes of energy and potential enstrophy in rotating stratified Boussinesq flows

H. Aluie[1,2(a)] and S. Kurien[2,3]

[1] *Center for Nonlinear Studies, Los Alamos National Laboratory - Los Alamos, NM 87545, USA*
[2] *Applied Mathematics and Plasma Physics (T-5), Theoretical Division, Los Alamos National Laboratory Los Alamos, NM 87545, USA*
[3] *New Mexico Consortium - Los Alamos, NM 87544, USA*

received 25 July 2011; accepted in final form 29 September 2011
published online 11 November 2011

PACS 47.27.-i – Turbulent flows
PACS 47.55.Hd – Stratified flows
PACS 47.32.Ef – Rotating and swirling flows

Abstract – We employ a coarse-graining approach to analyze non-linear cascades in Boussinesq flows using high-resolution simulation data. We derive budgets which resolve the evolution of energy and potential enstrophy simultaneously in space and in scale. We then use numerical simulations of Boussinesq flows, with forcing in the large scales, and fixed rotation and stable stratification along the vertical axis, to study the inter-scale flux of energy and potential enstrophy in three different regimes of stratification and rotation: i) strong rotation and moderate stratification, ii) moderate rotation and strong stratification, and iii) equally strong stratification and rotation. In all three cases, we observe constant fluxes of both global invariants, the mean energy and mean potential enstrophy, from large to small scales. The existence of constant potential enstrophy flux ranges provides the first direct empirical evidence in support of the notion of a cascade of potential enstrophy. The persistent forward cascade of the two invariants reflects a marked departure of these flows from two-dimensional turbulence.

Introduction. – The Kolmogorov [1] and Kraichnan [2] theories of three- and two-dimensional Navier-Stokes turbulence have served as a benchmark in the understanding of fluid turbulence and as fundamental tests for the accuracy of simulations. The Boussinesq approximation of the compressible Navier-Stokes equations in a rotating frame gives a fairly accurate description of the flow dynamics over much of the Earth's oceans and atmosphere but is prohibitively expensive to simulate in detail over global scales. Guided by the success of the Kolmogorov/Kraichnan theories, it would be useful to develop a statistical phenomenology of the small scales of Boussinesq flows to gain an understanding of the physics, serve as benchmarks to test simulations, and offer parameterizations which could eventually be useful in practical modeling of geophysical flows. In addition to global energy, the inviscid Boussinesq equations conserve local potential vorticity (hereafter PV) and global potential enstrophy, thus offering more complexity than incompressible Navier-Stokes dynamics. Charney [3] addressed one limiting case of the Boussinesq approximation, namely the quasi-geostrophic limit of strong rotation and strong stratification, and showed that the conservation of both energy and the quadratic potential enstrophy in such flows constrained energy to cascade to the large scales as in 2D turbulence [2].

Conservation of potential enstrophy is believed to play a fundamental role in the dynamics of the atmosphere and oceans [4]. Understanding its function in non-linear scale interactions would appear to be essential for extending Kolmogorov's theory to Boussinesq flows with rotation and stratification. Herring *et al.* [5] studied the cascade properties of potential enstrophy in turbulence simulations with a passive scalar in the absence of rotation and stratification. They concluded that because potential enstrophy in their simulation is not a quadratic, but a quartic invariant, the usual Kolmogorov-like arguments for a cascade and an inertial range do not apply. In fact, their potential enstrophy budget shows the direct action of viscous-diffusion terms at *all scales*, even in the limit of very small viscosity and diffusivity. Their fig. 15 shows that potential enstrophy dissipation peaks at the largest

(a) E-mail: hussein@jhu.edu

scales (see also their fig. 14 and the discussion on pp. 37 and 43). Thus, a pure inertial range of potential enstrophy flux is precluded because of contamination by dissipation at all scales. However, in Boussinesq flows, with strong rotation and/or strong stratification, Kurien *et al.* [6] (hereafter KSW06) derived analytically, starting from the evolution of the two-point correlation of potential vorticity, a flux law for potential enstrophy which is analogous to Kolmogorov's 4/5-law for energy flux in 3D incompressible turbulence. The so-called 2/3-law of KSW06 implies that an inertial cascade of potential enstrophy can exist in three limiting cases: i) strong rotation with moderate stratification; ii) moderate rotation with strong stratification; and iii) strong rotation and strong stratification. By "moderate" we mean that the rotation (stratification) frequency is of the same order as the non-linear turbulence frequency; whereas by "strong" we mean that the respective frequencies are much faster than the non-linear timescale. In the above three regimes, KSW06 showed that potential enstrophy, generally a quartic quantity, becomes quadratic which results in the localization of viscous-diffusion terms to the smallest scales, thus allowing for an inertial range of scales dominated by the flux of potential enstrophy. Furthermore, KSW06 suggested that in the absence of strong rotation and/or strong stratification, when potential enstrophy reverts to being quartic, viscous-diffusion effects may contaminate all scales, in agreement with the conclusions of [5].

The existence of an inertial cascade range for potential enstrophy is far from obvious and remains an unsettled issue. To date, there has been no empirical demonstration of KSW06's results on the constant flux range of potential enstrophy in Boussinesq flows. In [7] a phenomenology and supporting data from Boussinesq simulations with equally strong (non-dimensional) rotation and stratification were presented to show that conservation of quadratic potential enstrophy could constrain the spectral distribution of energy in the large wave numbers. In [8] the analysis and phenomenology of [7] was extended to include the two other limiting cases i) and ii) above, to show that indeed in all parameter regimes with linear PV, the downscale flux of (quadratic) potential enstrophy can constrain the scale distribution of energy. While the two studies [7,8] did not measure potential enstrophy flux, their numerical findings confirmed phenomenologically predicted scalings of the energy spectra assuming constant downscale fluxes of potential enstrophy. Motivated partially by those results, the present work uses data from [8] to directly measure the cascade of potential enstrophy for the first time.

Some previous studies have highlighted the interest in energy fluxes. The results from [9,10] of purely stratified flow computed in small-aspect-ratio domains with forcing of the horizontal velocity only, did not show convincing constant energy fluxes (see fig. 18 of [9] and fig. 15 of [10] which plot energy flux on a log-log scale). On the other hand [11] provides evidence of scale-independent fluxes of kinetic and potential energy in purely stratified flow in unit aspect ratio. It should be noted that these studies used forcing, stratification, and domain aspect ratio different from ours. Furthermore, the simulations of [9–11] were not reported to be in the linear PV regime and, therefore, our results may not apply to their flows. Most importantly, none of these previous studies computed or analyzed the potential enstrophy flux, which constitutes an essential part of our work.

In this letter, we present a very general framework for analyzing non-linear scale interactions in Boussinesq flows. The coarse-graining approach we utilize allows for probing the dynamics simultaneously in space and in scale. Motivated by the work of [6–8], we then measure fluxes of energy and potential enstrophy across scales from simulations in three distinct limits of rotation and stratification. Our results show constant and positive fluxes of the two quadratic invariants, indicating simultaneous persistent downscale cascades of both quantities in all three cases. Our measurements of potential enstrophy flux are a novel contribution of this letter and constitute the first empirical confirmation of analytical results by [6]. Furthermore, our evidence of a scale-independent energy flux is significant because it conveys that a cascade should persist to arbitrarily small scales at asymptotically high simulation resolutions.

Boussinesq dynamics. – We study stably stratified Boussinesq flows in a rotating frame. The dynamics is described by momentum (1) and active scalar (2) equations:

$$\partial_t \mathbf{u} + (\mathbf{u}\cdot\boldsymbol{\nabla})\mathbf{u} = -\boldsymbol{\nabla}p - f\hat{\mathbf{z}}\times\mathbf{u} - N\theta\hat{\mathbf{z}} + \nu\nabla^2\mathbf{u} + \boldsymbol{\mathcal{F}}^u, \quad (1)$$

$$\partial_t\theta + (\mathbf{u}\cdot\boldsymbol{\nabla})\theta = Nu_z + \kappa\nabla^2\theta + \mathcal{F}^\theta. \quad (2)$$

Here, $\mathbf{u}$ is a solenoidal velocity field, $\boldsymbol{\nabla}\cdot\mathbf{u}=0$, whose vertical component is u_z. The effective pressure is p, and $\boldsymbol{\mathcal{F}}^u$, $\mathcal{F}^\theta$ are external forces. Gravity, g, is constant and in the $-\hat{\mathbf{z}}$ direction. The total density is given by $\rho_T(\mathbf{x}) = \rho_0 - bz + \rho(\mathbf{x})$, such that $|\rho(\mathbf{x})| \ll |bz|$ and $|\rho(\mathbf{x})| \ll \rho_0$, where ρ_0 is a constant background density, b is constant and positive for stable stratification, and $\rho(\mathbf{x})$ is the fluctuating density field with zero mean. The normalized density, $\theta(\mathbf{x}) = \sqrt{g/b\rho_0}\rho(\mathbf{x})$, has units of velocity. For a constant rotation rate Ω about the z-axis, the Coriolis parameter is $f=2\Omega$. The Brunt-Väisälä frequency is $N=\sqrt{gb/\rho_0}$, the kinematic viscosity is $\nu=\mu/\rho_0$, and the mass diffusivity is κ. In this paper, we only study flows with Prandtl number $Pr=\nu/\kappa=\mathcal{O}(1)$. Relevant non-dimensional parameters are the Rossby number, $Ro=f_{nl}/f$, and the Froude number, $Fr=f_{nl}/N$, where we define the characteristic non-linear frequency as $f_{nl}=(\epsilon_f k_f^2)^{1/3}$, for a given energy injection rate ϵ_f at wave number k_f (see [6,8,12]).

The dynamics of inviscid and unforced Boussinesq flows (such that $\nu=\kappa=\mathcal{F}^\theta=\mathcal{F}_i^u=0$) is constrained by the conservation of potential vorticity, $q(\mathbf{x}) = \frac{N}{b}\boldsymbol{\omega}_a\cdot\boldsymbol{\nabla}\rho_T$, following material flow particles, $D_t q = \partial_t q + (\mathbf{u}\cdot\boldsymbol{\nabla})q = 0$. Here, the absolute vorticity is $\boldsymbol{\omega}_a = \boldsymbol{\omega} + f\hat{\mathbf{z}}$ and the local

Table 1: Parameters of the Boussinesq simulation data.

Run	Resolution	$f\,(Ro)$	$N\,(Fr)$
Rs	640^3	3000 (0.002)	14 (0.4)
rS	640^3	14 (0.4)	3000 (0.002)
RS	640^3	3000 (0.002)	3000 (0.002)

vorticity is $\boldsymbol{\omega} = \boldsymbol{\nabla}\times\mathbf{u}$. PV may be written in terms of $\boldsymbol{\omega}$ and θ as

$$q(\mathbf{x}) = f\partial_z\theta - N\boldsymbol{\omega}\cdot\hat{\mathbf{z}} + \boldsymbol{\omega}\cdot\boldsymbol{\nabla}\theta - fN. \tag{3}$$

The first two terms are linear and dominate over the quadratic term, $\boldsymbol{\omega}\cdot\boldsymbol{\nabla}\theta$, in the limit of large f and/or large N. The constant part in (3) does not participate in the dynamics and can, therefore, be neglected [12].

In addition to conservation of PV, the flow is constrained by the global conservation of potential enstrophy, $Q = \frac{1}{2}q^2$, such that $\frac{\mathrm{d}}{\mathrm{d}t}\langle Q\rangle = 0$, where $\langle\ldots\rangle = \frac{1}{V}\int_V \mathrm{d}^3\mathbf{x}(\ldots)$ is a space average. Another quadratic invariant of the inviscid dynamics is the total mean energy, $E_T = \frac{1}{2}\langle|\mathbf{u}|^2 + |\theta|^2\rangle$, such that $\frac{\mathrm{d}}{\mathrm{d}t}E_T = 0$.

Numerical data. – The Sandia-LANL DNS code was used to perform pseudo-spectral calculations of the Boussinesq equations (1), (2) on grids of 640^3 points in unit aspect ratio domains. The time stepping is 4th-order Runge-Kutta and the fastest linear wave frequencies are resolved with at least five time steps per wave period. The diffusion of both momentum and density (scalar) is modeled by hyperviscosity of Laplacian to the 8th power. The coefficient of the hyperviscous diffusion term is chosen dynamically such that the energy in the largest wave number shell (smallest resolved scale) is dissipated at each time step [12,13]. This choice ensures that one does not have to guess the coefficient *a priori* and is a way to allow the flow itself to determine the magnitude of the diffusion. Hyperviscosity is a standard dissipation model that has long been used in studies of rotating and/or stratified flows [9–12]. In principle, hyperviscosity can lead to thermalization and isotropy at the smallest scales [14]; however our results on the inertial-range cascades are robust and unaffected by the small-scale dissipation model [15]. Stochastic forcing is incompressible and equipartitioned between the three velocity components and θ. The forcing spectrum is peaked at $k_f = 4\pm1$, for large-scale forcing. We use the two-thirds dealiasing rule. These data were reported in [7,8], where further computational details may be found.

We analyze three sets of simulations corresponding to three extreme flow regimes summarized in table 1. The first, Rs, is a flow under strong rotation and moderate stratification, $f/N \gg 1$. The second, rS, is a flow under moderate rotation but strong stratification, $f/N \ll 1$. The third, RS, is a flow under strong rotation and strong stratification such that $f = N$. Figure 1 shows that in all three cases, $\langle Q\rangle$ is well approximated by (one-half) the square of the corresponding linear PV to within 3% or better (see [6,8]). Figure 1 gives evidence that our simulations are in regimes of strong rotation and/or strong stratification. We analyze snapshots of the flow at late times when $\langle Q\rangle$ along with small-scale energy spectra (at wave numbers $k \geqslant 6$) have reached a statistically steady state. The total energy, however, continues to grow due to an accumulation at the largest scales.

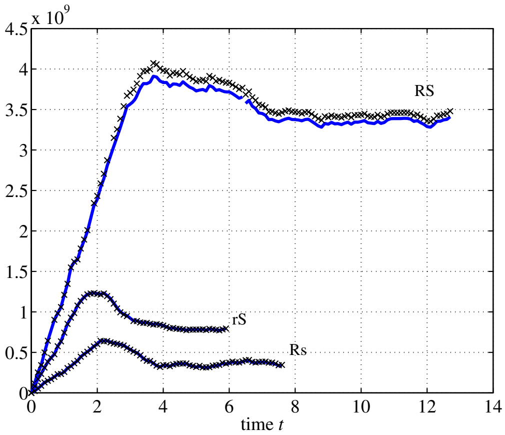

Fig. 1: (Colour on-line) Time series of mean potential enstrophy $\langle Q\rangle$ (solid line), and its quadratic part $\langle\widetilde{Q}\rangle$ (crosses). In run RS $\langle\widetilde{Q}\rangle = \langle[f\partial_z\theta - N\boldsymbol{\omega}\cdot\hat{\mathbf{z}}]^2\rangle/2$; in run rS $\langle\widetilde{Q}\rangle = \langle[N\boldsymbol{\omega}\cdot\hat{\mathbf{z}}]^2\rangle/2$; and in run Rs $\langle\widetilde{Q}\rangle = \langle[f\partial_z\theta]^2\rangle/2$. The plots show that $\langle Q\rangle$ reaches a steady state and that $\langle Q\rangle \simeq \langle\widetilde{Q}\rangle$ in all three regimes considered.

Analyzing the cascades by coarse-graining. – Following [16–19], we use a simple filtering technique common in the large eddy simulation (LES) literature to resolve turbulent fields simultaneously in scale and in space. Other decompositions, such as wavelet analysis, also allow for the simultaneous space-scale resolution and may be used to analyze non-linear scale interactions as well. We define a coarse-grained or (low-pass) filtered field in d dimensions as

$$\overline{\mathbf{a}}_\ell(\mathbf{x}) = \int \mathrm{d}^d\mathbf{r}\; G_\ell(\mathbf{r})\mathbf{a}(\mathbf{x}+\mathbf{r}), \tag{4}$$

where $G(\mathbf{r})$ is a normalized convolution kernel, $\int \mathrm{d}^d\mathbf{r}\,G(\mathbf{r}) = 1$. An example of such a kernel is the Gaussian function, $G(r) = \frac{1}{\sqrt{2\pi}}e^{-r^2/2}$. Its dilation $G_\ell(\mathbf{r}) \equiv \ell^{-d}G(\mathbf{r}/\ell)$ in d dimensions has its main support in a ball of radius ℓ. Operation (4) may be interpreted as a local space average. In the rest of our letter, we shall omit subscript ℓ whenever there is no ambiguity.

Applying the filtering operation (4) to the dynamics (1), (2) yields coarse-grained equations that describe the evolution of $\overline{\mathbf{u}}_\ell(\mathbf{x})$ and $\overline{\theta}_\ell(\mathbf{x})$ at every point $\mathbf{x}$ in space and at any instant of time:

$$\begin{aligned}\partial_t\overline{\mathbf{u}} + (\overline{\mathbf{u}}\cdot\boldsymbol{\nabla})\overline{\mathbf{u}} &= -\boldsymbol{\nabla}\overline{p} - f\hat{\mathbf{z}}\times\overline{\mathbf{u}} - N\overline{\theta}\hat{\mathbf{z}}\\ &\quad -\boldsymbol{\nabla}\cdot\overline{\tau}(\mathbf{u},\mathbf{u}) + \nu\nabla^2\overline{\mathbf{u}} + \overline{\boldsymbol{\mathcal{F}}^u},\end{aligned} \tag{5}$$

$$\begin{aligned}\partial_t\overline{\theta} + (\overline{\mathbf{u}}\cdot\boldsymbol{\nabla})\overline{\theta} &= N\,\overline{u}_z - \boldsymbol{\nabla}\cdot\overline{\tau}(\mathbf{u},\theta)\\ &\quad +\kappa\nabla^2\overline{\theta} + \overline{\mathcal{F}^\theta},\end{aligned} \tag{6}$$

where *subgrid stresses*, $\overline{\tau}_\ell(f,g)\equiv\overline{fg}_\ell-\overline{f}_\ell\,\overline{g}_\ell$, are "generalized 2nd-order moments" [17] accounting for the influence of eliminated fluctuations at scales $<\ell$.

The coarse-grained equations describe flow at scales $>\ell$, for arbitrary ℓ. The approach, therefore, allows for the simultaneous resolution of dynamics *both in scale and in space*. Furthermore, the approach admits intuitive physical interpretation of various terms in the coarse-grained balance (5), (6) which resemble the original governing equations (1), (2), except for additional *subgrid* terms which quantify the non-linear coupling between resolved and filtered scales. These subgrid terms depend inherently on the unresolved dynamics which has been filtered out. Traditional modeling efforts, such as in LES (see, for example, [20]), focus on devising closures for such terms which are plausible but whose regimes of applicability and validity are inevitably unknown. A key feature of the formalism employed here that distinguishes it from those modeling efforts is that it allows us to estimate the contribution of subgrid terms as a function of the resolution scale ℓ through exact mathematical analysis and direct numerical simulations (see, for example, [21–24]). Our approach thus quantifies the coupling that exists between different scales and may be used to extract certain scale-invariant features in the dynamics.

Large-scale energy budget. From eqs. (5) and (6), it is straightforward to derive an energy budget for the large scales, which reads

$$\partial_t\left(\frac{|\overline{\mathbf{u}}|^2}{2}+\frac{|\overline{\theta}|^2}{2}\right)+\boldsymbol{\nabla}\cdot\mathbf{J}_\ell = -\Pi_\ell-\nu|\boldsymbol{\nabla}\overline{\mathbf{u}}|^2-\kappa|\boldsymbol{\nabla}\overline{\theta}|^2 +\overline{\mathbf{u}}\cdot\overline{\boldsymbol{\mathcal{F}}^u}+\overline{\theta}\ \overline{\mathcal{F}^\theta}. \tag{7}$$

Here, $\nu|\boldsymbol{\nabla}\overline{\mathbf{u}}|^2+\kappa|\boldsymbol{\nabla}\overline{\theta}|^2$ is the molecular dissipation acting on scales $>\ell$, and $\overline{\mathbf{u}}\cdot\overline{\boldsymbol{\mathcal{F}}^u}+\overline{\theta}\ \overline{\mathcal{F}^\theta}$ is the energy injected due to external stirring. $\mathbf{J}_\ell(\mathbf{x})$ represents the space transport of large-scale energy whose complete expression is deferred to [15]. Subgrid scale (SGS) flux, $\Pi_\ell(\mathbf{x})$, accounts for the non-linear transfer of energy from scales $>\ell$ to smaller scales:

$$\Pi_\ell(\mathbf{x})=-\partial_j\overline{u}_i\overline{\tau}(u_i,u_j)-\partial_j\overline{\theta}\ \overline{\tau}(\theta,u_j). \tag{8}$$

The SGS flux in (8) is work done by large-scale velocity and scalar gradients, $\boldsymbol{\nabla}\overline{\mathbf{u}}(\mathbf{x})$ and $\boldsymbol{\nabla}\overline{\theta}(\mathbf{x})$, against subgrid stresses. It acts as a sink in the large-scale budget (7) and accounts for the energy transferred across scale ℓ at any point $\mathbf{x}$ in the flow. Furthermore, $\Pi_\ell(\mathbf{x})$ is Galilean invariant. Other definitions of a flux are possible, such as $\Pi_\ell(\mathbf{x})=\overline{u}_iu_j\partial_j(u_i-\overline{u}_i)$ (eq. (2.52) in [25]), which differs from our definition (8) by a total gradient (disregarding the scalar part). However, these alternate definitions are not pointwise Galilean invariant, so the amount of energy cascading at any point $\mathbf{x}$ in the fluid according to such definitions would depend on the observer's velocity.

Another physical requirement on the SGS flux $\Pi_\ell(\mathbf{x})$ is that it should vanish in the absence of fluctuations at scales smaller than ℓ [21,22]. For example, when $\ell=K_{max}^{-1}$, where K_{max} is the maximum wave number in a pseudospectral simulation, there should be no cascade across ℓ simply because fluctuations at wave vectors $|\mathbf{k}|>K_{max}$ have zero amplitude. This is satisfied by our definition (8) identically at every point $\mathbf{x}$ in the flow. Alternate definitions such as $\Pi_\ell(\mathbf{x})=\overline{u}_iu_j\partial_ju_i$ (eq. (6) in [26]) fail this pointwise requirement of a flux.

Large-scale Q budget. Similar to the momentum, scalar, and energy equations (5), (7), we can write down large-scale balances for PV and Q. The "bare" PV equation with diffusion and external forcing may be derived from eqs. (1) and (2) as

$$\partial_tq+(\mathbf{u}\cdot\boldsymbol{\nabla})q = \nu(\boldsymbol{\nabla}\theta-N\hat{\mathbf{z}})\cdot\nabla^2\boldsymbol{\omega}_a+\kappa\boldsymbol{\omega}_a\cdot\nabla^2\boldsymbol{\nabla}\theta +(\boldsymbol{\nabla}\theta-N\hat{\mathbf{z}})\cdot\boldsymbol{\mathcal{F}}^\omega+\boldsymbol{\omega}_a\cdot\boldsymbol{\nabla}\mathcal{F}^\theta, \tag{9}$$

where $\boldsymbol{\mathcal{F}}^\omega=\boldsymbol{\nabla}\times\boldsymbol{\mathcal{F}}^u$. Applying the filtering operation to (9) in the limit of strong rotation and/or stratification (limit of large f and/or N such that PV is linear, $q=f\partial_z\theta-N\omega_z$) yields the following balance for large-scale PV:

$$\partial_t\overline{q}+(\overline{\mathbf{u}}\cdot\boldsymbol{\nabla})\overline{q} = -\boldsymbol{\nabla}\cdot\overline{\tau}(q,\mathbf{u})-\nu\,N\,\nabla^2\overline{\omega}_z+\kappa\,f\,\nabla^2\partial_z\overline{\theta} -N\,\overline{\mathcal{F}^\omega}_z+f\,\partial_z\overline{\mathcal{F}^\theta}. \tag{10}$$

Using (10), we can now write the large-scale potential enstrophy budget in the limit of linear PV,

$$\partial_t\frac{|\overline{q}|^2}{2}+\boldsymbol{\nabla}\cdot\mathbf{J}^Q=-\Pi^Q-D^Q+\epsilon^Q_{inj}, \tag{11}$$

where $\mathbf{J}^Q(\mathbf{x})$ is the space transport, $D^Q_\ell(\mathbf{x})$ is the dissipation due to viscosity and diffusivity acting directly on scales $>\ell$, and ϵ^Q_{inj} is the potential enstrophy injected due to external forcing. These terms are defined in [15]. $\Pi^Q_\ell(\mathbf{x})$ is SGS flux of potential enstrophy,

$$\Pi^Q_\ell(\mathbf{x})=-\partial_j\overline{q}\ \overline{\tau}(q,u_j). \tag{12}$$

It is straightforward to verify that $\Pi^Q_\ell(\mathbf{x})$ is Galilean invariant and vanishes in the absence of subgrid fluctuations.

Calculating fluxes using sharp spectral filter. – We choose the so-called "sharp spectral filter" as our coarse-graining kernel in the definition of fluxes. We denote a field in a periodic domain $[0,1)^3$, coarse-grained with the spherically symmetric sharp-spectral filter to retain only Fourier modes $|\mathbf{k}|<K$, by

$$\mathbf{a}^{<K}(\mathbf{x})\equiv\sum_{|\mathbf{k}|\leqslant K}\hat{\mathbf{a}}(\mathbf{k})e^{i2\pi\mathbf{k}\cdot\mathbf{x}}. \tag{13}$$

This is similar to $\overline{\mathbf{a}}_\ell(\mathbf{x})$ with $\ell\sim K^{-1}$. We omit the factor 2π in reference to wave number in this letter. While an isotropic filter such as (13) cannot distinguish between different directions, it does not average out anisotropy if present in a flow as will be clearly demonstrated in [15].

Using this filter, we can discern the amount of energy and potential enstrophy cascading across a certain wave number K. For example, to analyze the energy cascade, we can compute

$$\Pi_K(\mathbf{x}) = -\partial_j u_i^{<K} \tau^{<K}(u_i, u_j) - \partial_j \theta^{<K} \tau^{<K}(\theta, u_j) \quad (14)$$

as a function of K. Here, $\tau^{<K}(f,g) = (fg)^{<K} - f^{<K} g^{<K}$. We can also analyze potential enstrophy cascade using

$$\Pi_K^Q(\mathbf{x}) = -\partial_j q^{<K} \tau^{<K}(q, u_j). \quad (15)$$

SGS energy flux (14) coincides with that used in [9,10] only after space averaging. Yet, our quantity has the correct pointwise physical properties discussed above and, therefore, allows for studying spatial properties of the cascades.

Numerical results. – In this letter, we restrict our numerical investigation to spatially averaged fluxes using the sharp spectral filter. Figure 2 shows that there is a positive and constant flux (y-axis shown on a linear scale to highlight true constancy) of total energy to small scales in all three cases of rotation and stratification[1]. While all three cases show a clear downscale energy cascade, the RS case also has a negative flux over $K \leqslant 4$ possibly indicative of the expected inverse cascade present in such regime (*e.g.*, [27–29]). We do not have the required scale range in our simulations to say anything more definitive about the dynamics at scales larger than that of forcing.

We wish to emphasize the constancy of fluxes. A constant flux indicates a *persistent* non-linear transfer of energy to smaller scales, *i.e.* the flow is able to sustain a cascade to *arbitrarily small scales*, regardless of how small the viscous-diffusion parameters are. The term "cascade" necessitates a flux constant in wave number. It is certainly possible for non-linear interactions to yield a transient transfer to smaller scales but one which does not persist (decays to zero) and cannot carry the energy all the way to molecular scales. This is sometimes observed, for example, in 2D turbulence simulations and experiments (*e.g.*, fig. 1 in [30]), where we know that a positive downscale flux of energy is only transient and cannot be constant (*e.g.*, fig. 1 in [31]). Such distinction between transient and constant fluxes is imperative to modeling efforts. In the former case, there is no cascade or enhancement of dissipation due to turbulence whereas in the latter case, dissipation becomes independent of the Reynolds number.

This issue is especially important when drawing conclusions from limited resolution simulations, true of most cases, including ours. A constant flux indicates that dissipation should be independent of the simulation resolution. One may contend that a constant flux is just a consequence of a steady state and having forcing localized to the largest scales. However, it may very well be that the flow reaches

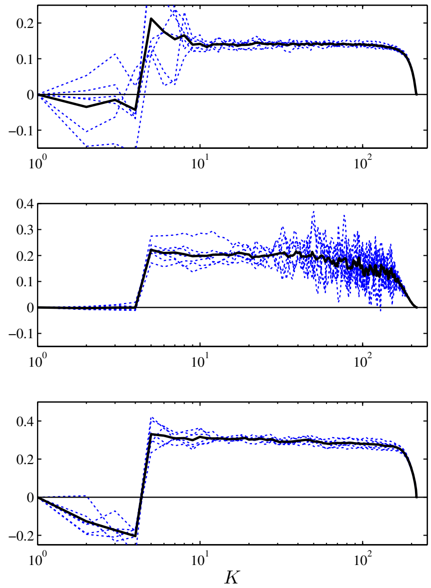

Fig. 2: (Colour on-line) Plots of total energy flux, $\langle \Pi_K \rangle$, from runs Rs (top), rS (middle), and RS (bottom). Dotted (blue) lines are fluxes taken from an instantaneous time snapshot. Solid (black) lines are averaged over time.

steady state due to direct viscous dissipation acting on all scales as shown in [5] for potential enstrophy rather than a Kolmogorov-like inertial cascade.

We also compute the potential enstrophy flux. Figure 3 shows that, in a manner similar to that of energy, there is a positive and constant flux of potential enstrophy in all three extreme cases[2]. The plots in fig. 3 are the first measurements of potential enstrophy flux in rotating stratified Boussinesq flows and constitute one of the main results in this letter. They can be regarded as the first empirical confirmation of analytical results in [6] which derived an exact law for potential enstrophy flux in physical space as a function of scale. Unlike for energy, $\langle \Pi_K^Q \rangle$ in fig. 3 for the RS case is not negative over $K \leqslant 4$.

Rotating and stratified flows are often said to be "two-dimensionalized" in some sense, eliciting comparisons with two-dimensional turbulence and often justifying the study of the latter as a simplified paradigm for geophysical flows. Here we point out that the existence of a concurrent flux of both energy and potential enstrophy in rotating and stratified flow to smaller scales is in itself a marked departure of these flows from 2D turbulence. In the latter case, it is known (*e.g.*, [2,31]) that the two cascades cannot co-exist over the same scale-range since a forward cascade of enstrophy acts as a constraint leading to an inverse cascade of energy to larger scales.

In rotating and stratified flows, the velocity and scalar fields can be decomposed into the sum of a vortical component, which accounts for all the potential vorticity in the flow, and into a wave component, which has zero

[1]The flux in the rS case is noisy at small scales because of a highly anisotropic cascade across wave vectors with large vertical component k_z while being entirely suppressed across modes with large horizontal component k_h [15]. The number of such anisotropic wave vectors does not increase with K and, therefore, does not provide the additional averaging needed to smooth out small-scale noise.

[2]The flux $\langle \Pi_K^Q \rangle$ in the rS case is noisy at small scales for the same reasons as in fig. 2 for $\langle \Pi_K \rangle$.

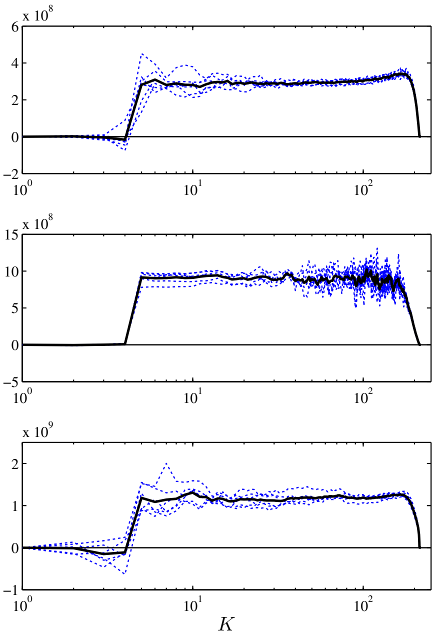

Fig. 3: (Colour on-line) Plots of potential enstrophy flux, $\langle\Pi_K^Q\rangle$, from runs Rs (top), rS (middle), and RS (bottom). Dotted (blue) lines are fluxes taken from an instantaneous time snapshot. Solid (black) lines are averaged over time.

potential vorticity (*e.g.*, [12,27]). In the strongly rotating and strongly stratified regime, it is known (see [27–29]) that the vortical component of the flow is governed by quasigeostrophic dynamics, which is very similar to 2D turbulence [3]. In this regime, a forward energy cascade of the vortical component is suppressed due to the forward cascade of potential enstrophy. We verified (to appear in [15]) that this is indeed the case in our RS run, where the forward energy cascade (in fig. 2, bottom panel) is due to the wave component of the flow in agreement with [27]. However, the situation in the remaining two cases, runs Rs and rS, is markedly different from both 2D and quasigeostrophic dynamics as will be discussed in [15].

Conclusions. – The two main results presented in this letter are i) energy and potential enstrophy budgets which resolve the dynamics simultaneously in space and in scale and ii) concurrent and persistent cascades of energy and potential energy to small scales in three extreme cases of rotating and stratified Boussinesq flow simulations. The numerical results on constant fluxes of potential enstrophy constitute the first direct empirical evidence in support of the analytical results by [6]. Our findings show a clear departure of the flows that we study from 2-dimensional turbulence and should be incorporated in any phenomenological treatments of strongly rotating and/or stratified Boussinesq flows. In a longer forthcoming work [15], we shall refine our analysis to study anisotropy of these cascades, their pointwise and scale locality properties, and quantify contributions from vortical and wave components.

* * *

We used resources of the Argonne Leadership Computing Facility at Argonne National Laboratory, supported by the Office of Science of the US DOE under Contract No. DE-AC02-06CH11357. HA acknowledges partial support from NSF grant PHY-0903872 during a visit to the Kavli Institute for Theoretical Physics. HA was supported by LANL/LDRD program and by DOE ASCR program in Applied Mathematical Sciences. SK received partial funding from NSF program Collaborations in the Mathematical Geosciences: NSF CMG-1025188. This research was performed under the auspices of the US DOE at LANL under Contract No. DE-AC52-06NA25396.

REFERENCES

[1] Kolmogorov A., *Dokl. Akad. Nauk SSSR*, **30** (1941) 9.
[2] Kraichnan R. H., *Phys. Fluids*, **10** (1967) 1417.
[3] Charney J. G., *J. Atmos. Sci.*, **28** (1971) 1087.
[4] Vallis G. K., *Atmospheric and Oceanic Fluid Dynamics* (Cambridge University Press) 2006.
[5] Herring J. R., Kerr R. M. and Rotunno R., *J. Atmos. Sci.*, **51** (1994) 35.
[6] Kurien S., Smith L. and Wingate B., *J. Fluid Mech.*, **555** (2006) 131.
[7] Kurien S., Wingate B. and Taylor M. A., *EPL*, **84** (2008) 24003.
[8] Kurien S., (2010) arXiv:1005.5366 unpublished.
[9] Lindborg E., *J. Fluid Mech.*, **550** (2006) 207.
[10] Brethouwer G., Billant P., Lindborg E. and Chomaz J.-M., *J. Fluid Mech.*, **585** (2007) 343.
[11] Waite M. L., *Phys. Fluids*, **23** (2011) 066602.
[12] Smith L. M. and Waleffe F., *J. Fluid Mech.*, **451** (2002) 145.
[13] Chasnov J. R., *Phys. Fluids*, **6** (1994) 1036.
[14] Frisch U. *et al.*, *Phys. Rev. Lett.*, **101** (2008) 144501.
[15] Aluie H. and Kurien S., in preparation (2011).
[16] Leonard A., *Adv. Geophys.*, **18** (1974) A237.
[17] Germano M., *J. Fluid Mech.*, **238** (1992) 325.
[18] Eyink G. L., *J. Stat. Phys.*, **78** (1995) 335.
[19] Eyink G. L., *Physica D*, **207** (2005) 91.
[20] Meneveau C. and Katz J., *Annu. Rev. Fluid Mech.*, **32** (2000) 1.
[21] Eyink G. and Aluie H., *Phys. Fluids*, **21** (2009) 115107.
[22] Aluie H. and Eyink G., *Phys. Fluids*, **21** (2009) 115108.
[23] Aluie H. and Eyink G., *Phys. Rev. Lett.*, **104** (2010) 081101.
[24] Aluie H., *Phys. Rev. Lett.*, **106** (2011) 174502.
[25] Frisch U., *Turbulence. The legacy of A. N. Kolmogorov* (Cambridge University Press, UK) 1995.
[26] Mininni P. D., Alexakis A. and Pouquet A., *Phys. Rev. E*, **77** (2008) 036306.
[27] Bartello P., *J. Atmos. Sci.*, **52** (1995) 4410.
[28] Babin A. *et al.*, *Theor. Comput. Fluid Dyn.*, **9** (1997) 223.
[29] Embid P. F. and Majda A. J., *Geophys. Astrophys. Fluid Dyn.*, **87** (1998) 1.
[30] Chen S. *et al.*, *Phys. Rev. Lett.*, **96** (2006) 084502.
[31] Boffetta G., *J. Fluid Mech.*, **589** (2007) 253.